

Expression of lymphotoxin beta governs immunity at two distinct levels

Tobias Junt¹, Alexei V. Tumanov², Nicola Harris¹, Mathias Heikenwalder³, Nicolas Zeller³, Dmitry V. Kuprash², Adriano Aguzzi³, Burkhard Ludewig⁴, Sergei A. Nedospasov² and Rolf M. Zinkernagel¹

¹ Institute of Experimental Immunology, Zürich, Switzerland

² Laboratory of Molecular Immunology, Engelhardt Institute of Molecular Biology, Moscow, Russia

³ Institute of Neuropathology, University Hospital of Zürich, Zürich, Switzerland

⁴ Research Department, Kantonsspital, St. Gallen, Switzerland

Interaction of lymphotoxin $\alpha_1\beta_2$ (LT $\alpha_1\beta_2$) with its receptor is key for the generation and maintenance of secondary lymphoid organ microstructure. We used mice conditionally deficient for LT β on different lymphocyte subsets to determine how the LT β -dependent lymphoid structure influences immune reactivity. All conditionally LT β -deficient mice mounted normal immune responses against vesicular stomatitis virus (VSV), and were protected against lymphocytic choriomeningitis virus (LCMV). In contrast, they exhibited reduced immune responses against non-replicating antigens. Completely LT β -deficient mice failed to retain VSV in the marginal zone and died from VSV infections, and they became virus carriers following infection with the non-cytopathic LCMV, which was correlated with defective virus replication in dendritic cells. It was ruled out that LT β expression on lymphocytes influenced their activation, homing capacity, or maturation. We therefore conclude that LT β expression influences immune reactivity at two distinct levels: (i) Expression of LT β on lymphocytes enhances the induction of immune responses against limiting amounts of antigen. (ii) Expression of LT β on non-lymphocytes governs antiviral immunity by enhancing antigen presentation on antigen-presenting cells. This prevents cytotoxic T lymphocytes exhaustion or death of the host by uncontrolled virus spread.

Received 11/1/06

Revised 5/5/06

Accepted 20/6/06

[DOI 10.1002/eji.200626255]

Key words:
Antibody · Cytotoxic T lymphocyte · Lymphoid structure · Virus infections

Introduction

The lymphotoxin (LT) signaling system plays an important role in lymphoid organogenesis [1]. Production of LT $\alpha_1\beta_2$ is crucial for the formation of secondary

lymphoid organ anlagen [2–4] and the expression of homeostatic chemokines [5]. Thus, LT α ^{-/-} mice [6, 7], LT β ^{-/-} mice [8, 9] and mice deficient for the LT β receptor (LT β R^{-/-}, [10]), lack Peyer's patches (PP) and most lymph nodes, and show morphological deficiencies of the spleen. Various attempts have been undertaken to determine both the source and the targets of LT $\alpha_1\beta_2$ in lymphoid organogenesis as well as its time window of action. CD4⁺CD3⁻IL-7R⁺ lymphoid tissue-inducing cells (LTIC) have been shown to express LT $\alpha_1\beta_2$ early during ontogeny of lymph nodes [3] and PP [11]. Later, during lymphoid organ development, B cells and T cells appear to be the primary source [12, 13]. The target cells for LT $\alpha_1\beta_2$ are, in most instances, stromal cells of mesenchymal origin [4], which can differentiate into T or B cell zone stromal cells.

Correspondence: Dr. Tobias Junt, CBR Institute of Biomedical Research, Harvard Medical School, 200 Longwood Ave., Boston, MA 02115, USA

Fax: +1-617-278-3030

e-mail: junt@cbri.institute.org

Abbreviations: **FDC:** follicular dendritic cell ·

LCMV: lymphocytic choriomeningitis virus · **LT:** lymphotoxin ·

LTIC: lymphoid tissue-inducing cell · **MLN:** mesenteric lymph

node · **MZ:** marginal zone · **PP:** Peyer's patch · **VSV:** vesicular

stomatitis virus

The structure of secondary lymphoid organs plays a role in determining the capacity of an organism to respond to antigens [14]. For example, $LT\beta^{-/-}$ mice and $LT\alpha^{-/-}$ mice, which display severe defects in lymphoid organ structure, are known to be highly susceptible to virus infections [15–17]. In contrast, mice with weaker structural alterations, e.g. of the T cell zone in mice deficient for CCR7 or its ligands [18, 19], or the B cell zone in mice deficient for CXCR5 [20], show only a minor impairment of antiviral immune responses. Therefore, these studies do not establish which degree of lymphoid organization is sufficient and which lymphoid microcompartments are necessary for the generation of antiviral immunity. As $LT\alpha_1\beta_2$ is the key inducer of lymphoid anlagen and constitutive chemokines, mice conditionally deficient for $LT\beta$ on distinct lymphocyte subsets permit the analysis of graded defects of lymphoid microarchitecture in the generation of adaptive immune responses. Here, we used mice with conditional inactivation of the $LT\beta$ gene in T cells (T- $LT\beta^{-/-}$), B cells (B- $LT\beta^{-/-}$), T and B cells (TB- $LT\beta^{-/-}$) or complete $LT\beta^{-/-}$ mice to determine how $LT\beta$ from T cells, B cells or non-T/non-B cells (e.g. NK cells, DC or LTIC) provides the morphological basis for immune reactivity against viruses and non-replicating antigens.

In contrast to $LT\beta^{-/-}$ mice, all cell-specifically $LT\beta$ -deficient mice were able to mount protective antiviral immune responses against viruses. However, none of these strains were able to respond to non-replicating antigens. In $LT\beta^{-/-}$ mice we found that virus could spread in an uncontrolled fashion, due to incomplete antigen retention in the spleen. These results suggest that $LT\beta$ regulates immunity at two levels: Expression of $LT\beta$ on T or B lymphocytes is crucial for the induction of adaptive immune responses against small amounts of antigen but dispensable for the induction of adaptive responses against replicating infectious agents. Expression of $LT\beta$ on cells other than T and B cells (i.e. NK cells, DC or LTIC) is key for antigen sampling by APC of the marginal zone (MZ) and by DC.

Results

Defective architecture but normal cellularity of secondary lymphoid organs in conditionally $LT\beta$ -deficient mice

Since $LT\alpha_1\beta_2$ plays an important role in the formation and maintenance of secondary lymphoid organs, we first characterized the structure of spleens and lymph nodes of $LT\beta$ -deficient mice. Mesenteric, inguinal, brachial, para-aortal, submandibular, mediastinal and popliteal lymph nodes and PP were present in C57BL/6, T- $LT\beta^{-/-}$, B- $LT\beta^{-/-}$ and TB- $LT\beta^{-/-}$, but not in $LT\beta^{-/-}$ mice, which

only exhibited one small, poorly segmented mesenteric lymph node (MLN) in 75% of the mice and no PP. Immunohistochemistry on spleen sections of these strains (Fig. 1A) revealed that T- $LT\beta^{-/-}$ mice showed a largely intact splenic morphology, with the exception of looser follicular dendritic cell (FDC) networks, as shown by FDC-M1 staining. B- $LT\beta^{-/-}$ mice had normal B and T cell zones, a rudimentary MZ and small, but still detectable FDC-M1⁺ networks. TB- $LT\beta^{-/-}$ mice lacked clearly demarcated T and B cell zones, but also organized MZ or FDC-M1⁺ networks. Networks of FDC within PNA-positive GC could not even be induced in TB- $LT\beta^{-/-}$, or augmented in B- $LT\beta^{-/-}$, following immunization of these mice with the potent B and T helper cell-activating antigen vesicular stomatitis virus (VSV) (Fig. 1B). $LT\beta^{-/-}$ mice exhibited a weak segregation of T and B cell zones, and the MZ and FDC networks were totally absent [21]. It is of note that these mice died between days 8 and 11 following VSV infection (see below).

With regard to the microanatomy of MLN (Fig. 2), T- $LT\beta^{-/-}$ mice did not exhibit obvious morphological defects. The only defect of B- $LT\beta^{-/-}$ and TB- $LT\beta^{-/-}$ mice was an impairment of FDC-M1⁺ clusters. $LT\beta^{-/-}$ mice additionally lacked MOMA-1⁺ cells of the subcapsular sinus, and had no clearly segregated T and B cell zones.

We next enumerated the cellular constituents of spleen, blood, inguinal lymph nodes and MLN of these animals by FACS (Fig. 3 and data not shown). Blood was of normal cellularity and lymph nodes and spleen were of normal size in all mice, except in $LT\beta^{-/-}$ mice, which lacked all lymph nodes except the MLN and had elevated numbers of leukocytes in peripheral blood. In addition, the cellular composition of spleen, lymph nodes and blood was most profoundly altered in $LT\beta^{-/-}$ mice. As expected, NK cells were almost undetectable in these mice [22]. $LT\beta$ -deficient DC precursors of the bone marrow can differentiate normally [23], but CD11c⁺CD11b⁺ myeloid DC show a homing defect to spleens of $LT\beta^{-/-}$ mice [24]. This was mirrored by increased numbers of DC in the blood of $LT\beta^{-/-}$ mice. Mice that lacked $LT\beta$ on T cells, i.e. the T- $LT\beta^{-/-}$ and TB- $LT\beta^{-/-}$ strains showed slightly reduced numbers of CD4⁺ and CD8⁺ T cells in blood and secondary lymphoid organs, compared to B- $LT\beta^{-/-}$. This may reflect the reduced export of mature T cells from the thymus in the absence of $LT\beta$ -signaling [25]. In $LT\beta^{-/-}$ mice this effect was likely masked by the general lymphocytosis.

In summary, lymph nodes and spleen of T-, B-, and TB- $LT\beta^{-/-}$ mice were relatively normal in terms of overall cell numbers. Minor alterations of the cellular composition of these organs and graded anomalies of lymphoid structure were detected. Morphological defects in $LT\beta^{-/-}$ mice, however, were more severe in that they lacked most lymph nodes, PP, MOMA⁺ metallo-

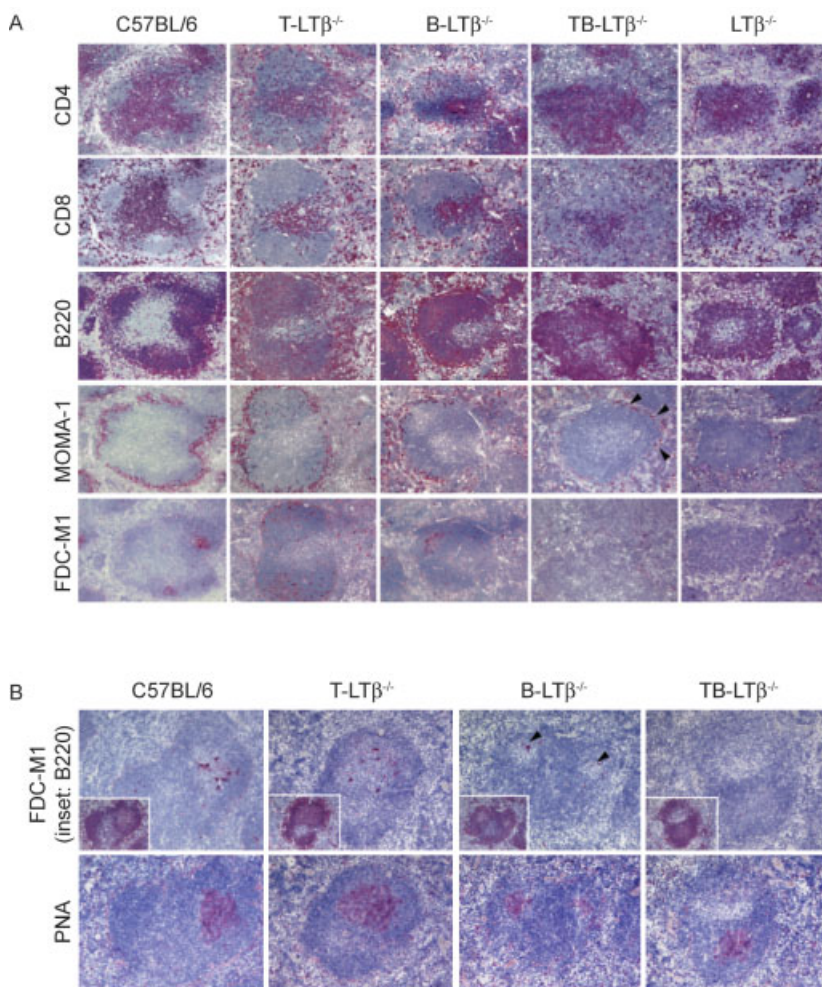


Fig. 1. Immunohistochemistry of spleens of LT-deficient mouse strains. (A) Immunohistochemistry of naive spleens. Arrowheads indicate the rudiment of the MZ in TB-LT $\beta^{-/-}$ mice. (B) Immunohistochemistry of spleens on day 14 following infection with 2×10^6 PFU VSV-IND i.v. Markers and mouse strains are indicated. Arrowheads indicate FDC in B-LT $\beta^{-/-}$ mice. Original magnification for all panels was 120x.

philic macrophages and ERTR9⁺ macrophages of the MZ (data not shown), and NK cells. Overall, the defects of lymphoid organ microanatomy of these mouse strains increased in severity as follows: C57BL/6 < T-LT $\beta^{-/-}$ < B-LT $\beta^{-/-}$ < TB-LT $\beta^{-/-}$ < LT $\beta^{-/-}$ (see also [13]).

Correlation of LT β expression in secondary lymphoid organs with integrity of lymphoid microstructure

Next, we determined whether the severity of morphological defects within secondary lymphoid organs correlated with the level of LT β expression. To this end, we quantified LT β mRNA in spleens and MLN of naive C57BL/6 mice, T-, B-, TB- and complete LT $\beta^{-/-}$ mice by real-time RT-PCR (Fig. 4A). The morphological defects correlated with reduced expression levels of LT β . It is thus likely that the aberrant microstructure of secondary lymphoid organs in these gene-targeted strains was due to a dose effect of LT β during ontogeny. Interestingly, less than 1% of the wild-type expression level still allowed the formation of all lymph node anlagen in TB-LT $\beta^{-/-}$ mice, whereas complete absence of

LT β expression in LT $\beta^{-/-}$ mice precluded the development of most lymph nodes. This difference in lymph node differentiation between TB-LT $\beta^{-/-}$ and LT $\beta^{-/-}$ mice was striking and may reflect the expression of LT β on LTIC of TB-LT $\beta^{-/-}$ but not of LT $\beta^{-/-}$ mice. Alternatively, it may point out to a role of LT β derived from another non-T non-B cell lineage in the formation of lymph node anlagen. In line with this notion, we have found LT β expression on NK cells and DC sorted from naive mice, but only weak expression on macrophages (Fig. 4B). NK cells, DC and macrophages expressed very low levels of LT α , whereas macrophages showed strong expression of TNF. LIGHT expression on most sorted cell types was absent, except on T cells and DC, where it was close to the level of detection (data not shown). To exclude locus control or secondary effects due to deregulation of LT β R or its ligands on mRNA expression levels, we analyzed expression levels of LT α , TNF or herpes virus entry mediator ligand (LIGHT) in spleens and MLN of LT $\beta^{-/-}$, B-LT $\beta^{-/-}$, T-LT $\beta^{-/-}$ and T/B-LT $\beta^{-/-}$ mice and C57BL/6 controls by real-time RT-PCR. Consistent with a previous report [21], we were not able to detect altered mRNA expression levels of LT α , TNF and LIGHT in spleens or

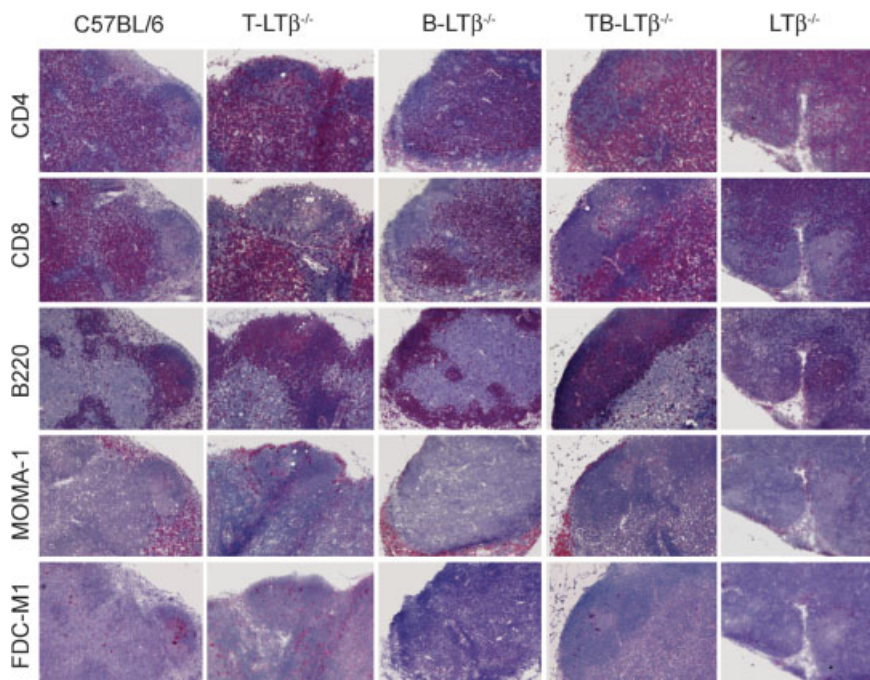


Fig. 2. Immunohistochemistry of MLN of $LT\beta$ -deficient mouse strains. Immunohistochemistry of MLN from naive mice. Markers and mouse strains are indicated. Original magnification was 120x.

MLN of $LT\beta$ -deficient mouse strains when compared to age-matched C57BL/6 controls, as indicated by not significantly changed $\Delta\Delta\text{Act}$ levels (<2 ; data not shown). The unique exception to the rule of unaltered expression levels of other gene products from the TNF/LT locus in $LT\beta$ -deficient mice were spleens of complete $LT\beta^{-/-}$ mice where we found a slight increase of $LT\alpha$, but not TNF or LIGHT expression.

Normal intrinsic T and B cell function in the absence of $LT\beta$

Expression of $LT\alpha_1\beta$ can be induced on the surface of activated T and B cells [26], possibly secondary to the activation-dependent induction of $LT\alpha$ [27]. Before studying immune responses in $LT\beta$ -deficient mice, we therefore wanted to exclude that deficient $LT\beta$ expres-

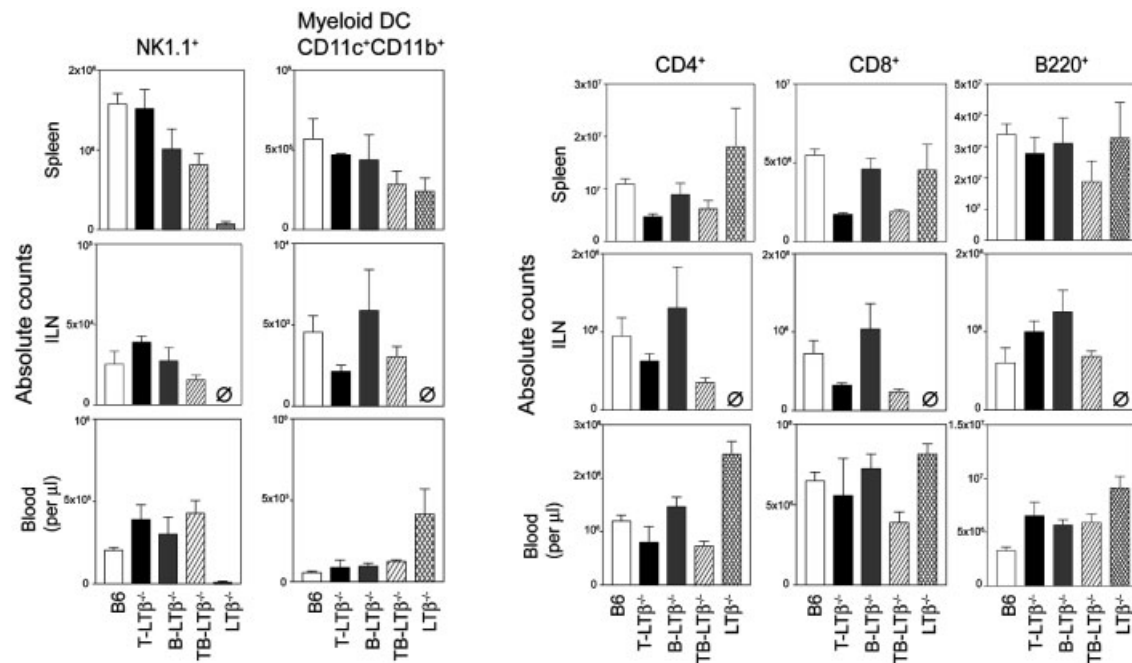


Fig. 3. Absolute cell counts of spleens, inguinal lymph nodes and blood of naive $LT\beta$ -deficient mouse strains. Spleens, both inguinal LN, or 100 μL of blood from naive C57BL/6 or $LT\beta$ -deficient mice were analyzed for the given markers by FACS. Bars represent means \pm SD of $n = 3\text{--}7$ mice.

sion influenced the costimulatory, proliferative, migratory or secretory activity of activated T and B cells. To this end, we stimulated MACS-purified CD43⁻ B cells for 3 days with anti-CD40 or LPS, and cytokines. LTβ-deficient B cells secreted IgM within normal levels (Fig. 5A) and expressed normal levels of CD80 and CD86 (Fig. 5B, upper and middle panel). The proliferative capacity of LTβ^{-/-} B cells was comparable to wild-type controls as assessed by CFSE proliferation assays (Fig. 5B, bottom panel). After 5 days of culture, LTβ^{-/-} B cells had switched their immunoglobulin

isotype as efficiently as wild-type controls (Fig. 5C). Next, we stimulated sorted CD4⁺ and CD8⁺ T cells of C57BL/6 mice or LTβ^{-/-} mice *in vitro*, on plate-bound anti-CD3 in the presence of anti-CD28 and IL-2. Compared to C57BL/6 mice, neither CD4⁺ nor CD8⁺ T cells from LTβ^{-/-} mice showed differences in the expression of activation markers (Fig. 5D) in their cytokine secretion pattern (Fig. 5E) and in their proliferative capacity (Fig. 5F). Finally, we compared the capacity of T and B lymphocytes from LTβ^{-/-} versus C57BL/6 mice to home within a correctly formed splenic microenvironment. For this purpose, 3 × 10⁶ MACS-sorted and CFSE-labeled T or B lymphocytes from LTβ^{-/-} or C57BL/6 mice were adoptively transferred to naive C57BL/6 mice. When the spleens of these mice were examined 6 h later, we observed a similar capacity of LTβ^{-/-} T cells to enter the T cell zones (Fig. 5G, upper row). Six hours after transfer, most LTβ^{-/-} and C57BL/6 B cells had entered B cell zones, while others were still detected in the red pulp (Fig. 5G, lower row). Overall, we conclude that LTβ-deficiency does not confer an intrinsic defect on lymphocyte activation, proliferation or migration to the T or B cell zones.

We additionally tested whether LTβ deficiency affected lymphocyte development. B cell development takes place in the BM, with the various developmental stages expressing distinct markers. The BM of LTβ^{-/-} mice was fractionated into subpopulations A–F by cytofluorimetry according to the classification by Hardy [28]. LTβ^{-/-} mice had normal frequencies of B cell precursors, when compared to C57BL/6 bone marrow (Fig. 6A, see legend for details). In addition, transitional and mature B cells were present in normal frequencies in spleens of LTβ^{-/-} mice (Fig. 6B). Thymus of LTβ^{-/-} mice had a normal cellular composition when compared to C57BL/6 mice, with only a mild elevation of single-positive cells (Fig. 6C). Therefore, LTβ^{-/-} deficiency did not cause an obvious developmental defect of T and B lymphocytes.

Deficient B cell responses in LT-deficient mice at low antigen doses

As shown above, LTβ-deficiency did not cause obvious defects in lymphocyte development or function at the single-cell level. The series of conditionally LTβ-targeted mice therefore permitted investigations of the role of stepwise reduced integrity of secondary lymphoid organ structure on antiviral immunity.

All LTβ-deficient mouse strains mounted early and strong virus neutralizing IgM titers following infection with 2 × 10⁶ PFU of VSV (Fig. 7A). Surprisingly, LTβ^{-/-} mice died between days 8 and 11 following infection whilst all other LTβ-deficient mice mounted comparable viral neutralizing IgG titers, in spite of their compro-

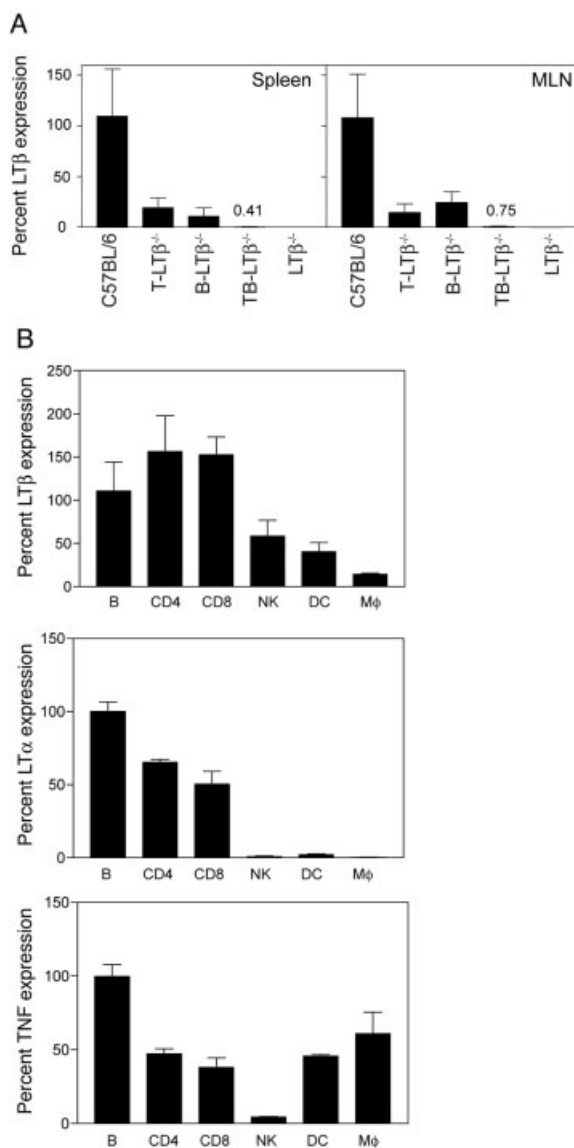


Fig. 4. Expression levels of LTβ mRNA in spleens, MLN and sorted cell populations. (A) SYBR-greenTM based real-time RT-PCR with LTβ expression levels of C57BL/6 mice set as 100% ($n = 2$ mice per group, PCR-reaction run in quadruplicates). Numbers represent means of LTβ expression in TB-LTβ^{-/-} mice in percent. (B) SYBR-greenTM based real-time RT-PCR of sorted cell populations from B6 mice with LTβ, LTα or TNF expression levels of B cells set as 100% (PCR run in triplicates).

mised lymphoid microstructure (Fig. 7B). As shown in Fig. 1B, VSV infection induced PNA-positive GC that were partially or completely devoid of FDC, in B-LT $\beta^{-/-}$ and TB-LT $\beta^{-/-}$ mice. It is thus possible that the maturation of virus-neutralizing IgG was impaired in these mice. Immunization with non-replicating UV-inactivated VSV virions (UV-VSV), or recombinant VSV-G, led to reduced IgM and IgG titers in all LT β -deficient

strains (Fig. 7A, B). These data indicated that a highly organized lymphoid architecture was dispensable for the generation of strong neutralizing antibody responses against live VSV. However, a high degree of lymphoid organization was necessary for the induction of T-independent and T-dependent B cell responses against non-replicating antigens such as UV-VSV or VSV-G.

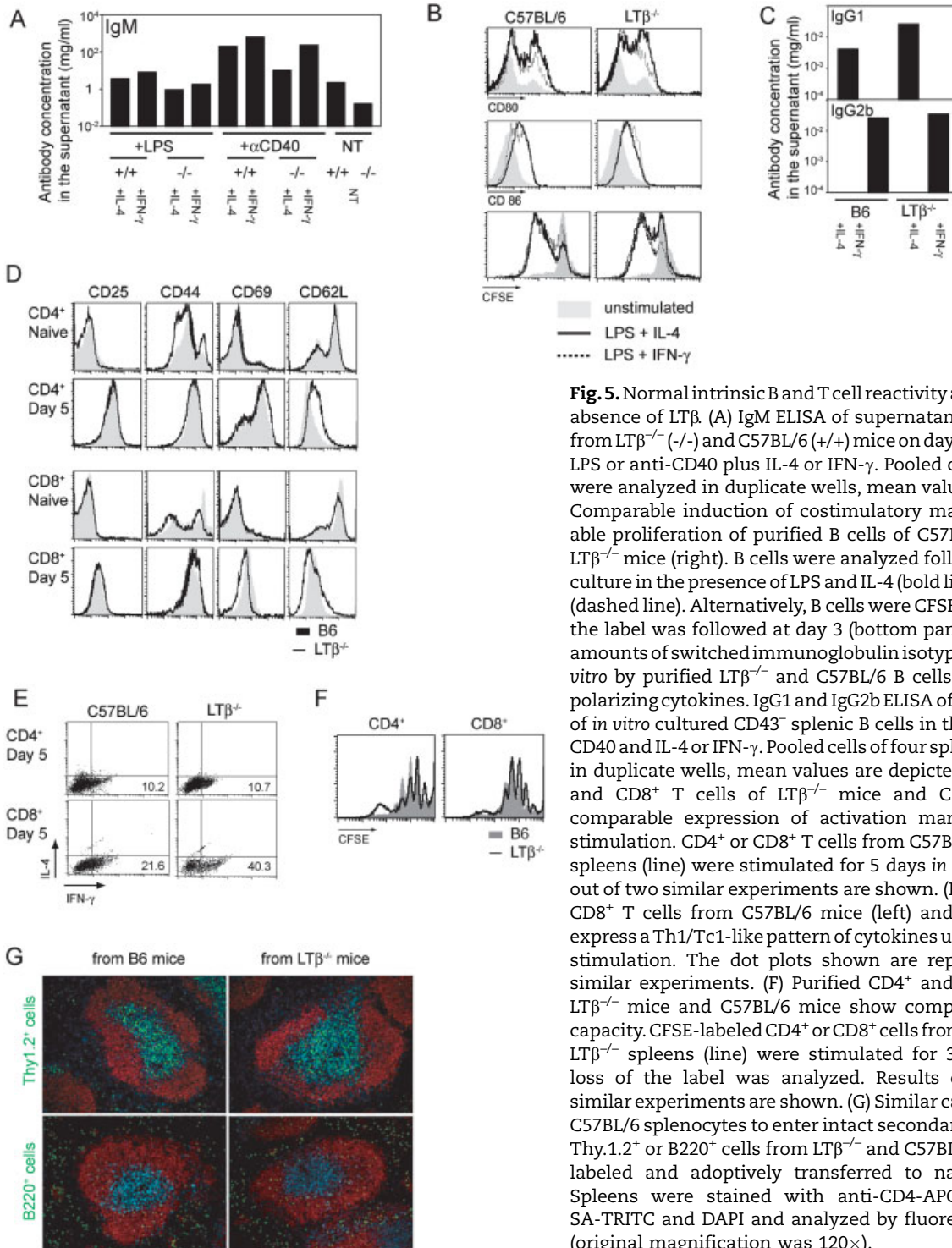


Fig. 5. Normal intrinsic B and T cell reactivity and migration in the absence of LT β . (A) IgM ELISA of supernatants of B cell cultures from LT $\beta^{-/-}$ (-/-) and C57BL/6 (+/+) mice on day 3 in the presence of LPS or anti-CD40 plus IL-4 or IFN- γ . Pooled cells of four spleens were analyzed in duplicate wells, mean values are depicted. (B) Comparable induction of costimulatory markers and comparable proliferation of purified B cells of C57BL/6 mice (left) and LT $\beta^{-/-}$ mice (right). B cells were analyzed following three days of culture in the presence of LPS and IL-4 (bold line) or LPS and IFN- γ (dotted line). Alternatively, B cells were CFSE-labeled and loss of the label was followed at day 3 (bottom panel); (C) Comparable amounts of switched immunoglobulin isotypes can be induced *in vitro* by purified LT $\beta^{-/-}$ and C57BL/6 B cells in the presence of polarizing cytokines. IgG1 and IgG2b ELISA of day 5 supernatants of *in vitro* cultured CD43⁻ splenic B cells in the presence of anti-CD40 and IL-4 or IFN- γ . Pooled cells of four spleens were analyzed in duplicate wells, mean values are depicted; (D) Purified CD4⁺ and CD8⁺ T cells of LT $\beta^{-/-}$ mice and C57BL/6 mice show comparable expression of activation markers upon *in vitro* stimulation. CD4⁺ or CD8⁺ T cells from C57BL/6 (shade) or LT $\beta^{-/-}$ spleens (line) were stimulated for 5 days *in vitro*. Results of one out of two similar experiments are shown. (E) Purified CD4⁺ and CD8⁺ T cells from C57BL/6 mice (left) and LT $\beta^{-/-}$ mice (right) express a Th1/Tc1-like pattern of cytokines upon 3 days of *in vitro* stimulation. The dot plots shown are representative of two similar experiments. (F) Purified CD4⁺ and CD8⁺ T cells from LT $\beta^{-/-}$ mice and C57BL/6 mice show comparable proliferative capacity. CFSE-labeled CD4⁺ or CD8⁺ cells from C57BL/6 (shade) or LT $\beta^{-/-}$ spleens (line) were stimulated for 3 days *in vitro*, and loss of the label was analyzed. Results of one out of two similar experiments are shown. (G) Similar capacity of LT $\beta^{-/-}$ and C57BL/6 splenocytes to enter intact secondary lymphoid organs. Thy1.2⁺ or B220⁺ cells from LT $\beta^{-/-}$ and C57BL/6 mice were CFSE-labeled and adoptively transferred to naive C57BL/6 mice. Spleens were stained with anti-CD4-APC, anti-B220-biotin, SA-TRITC and DAPI and analyzed by fluorescence microscopy (original magnification was 120 \times).

Reduced capture of VSV particles in the marginal zone of LT β -deficient mouse strains

Paradoxically, VSV infection was lethal in completely LT β -deficient mice in spite of normal titers of virus-neutralizing IgM at early time points following infection (see Fig. 7A). To rule out the possibility that the reduced number of lymph nodes was responsible for the lethality of VSV infections in LT β ^{-/-} mice, we generated LT β ^{-/-}→B6 BM chimeras. Eight weeks after reconstitution, these mice have normal numbers of lymph nodes and mounted normal titers of IgM early after infection (Fig. 7C), but still succumbed to VSV infections, whilst control B6→B6 chimeras survived. After VSV infection, virions are rapidly captured within the MZ *via* complement and natural antibodies [29]. T-LT β ^{-/-} mice captured VSV particles as efficiently as C57BL/6 mice, but B-LT β ^{-/-} and TB-LT β ^{-/-} mice showed a partial, and LT β ^{-/-} mice a complete impairment of VSV capture in the MZ (Fig. 7D). This correlated with the VSV titers detected in the spleen 24 h after infection (Fig. 7E). The capacity of LT β -deficient mice to fix VSV virions in the spleen therefore correlated to the integrity of the MZ, as indicated by the intensity of the MOMA-1 staining (see Fig. 1A). Similarly, B6→B6 BM chimeras, but not LT β ^{-/-}→B6 BM chimeras, had an intact MZ, to which VSV particles localized following infection (Fig. 7F). It has been observed previously that the failure to capture VSV particles within the MZ results in death of the host, as a result of systemic virus spread and virus replication in the brain [30]. This was confirmed in our system by infecting groups of four C57BL/6, B-LT β ^{-/-} and LT β ^{-/-} mice with 2×10^6 PFU VSV *i.v.* On day 10, *i.e.* by the time that two of the infected LT β ^{-/-} mice were taken out of the experiment due to signs of ascending paralysis, viral titers in CNS and peripheral organs were determined for all groups of mice. Live virus was detected in the brain and spinal cord of only the moribund, not the symptom-free LT β ^{-/-} mice (10^4 – 10^7 PFU/organ). Interestingly, all peripheral organs of moribund LT β ^{-/-} mice were free of virus. B-LT β ^{-/-} mice and B6 mice did not contain virus in any of the organs tested. These results strongly suggest that death of VSV-infected LT β ^{-/-} mice was due to the cytopathic effect of the virus in the CNS. The inability of LT β -deficient mice to cope with VSV infections is therefore likely to be caused by the insufficient capture of virus within the MZ allowing uncontrolled virus spread to neuronal tissue.

Reduced capacity to mount CTL responses but efficient antiviral protection in LT β -deficient mouse strains

We next assessed whether the LT β -deficient mouse strains showed impaired antiviral CTL responses. For this purpose, mice were infected with 200 PFU lymphocytic choriomeningitis virus (LCMV)-WE *i.v.* and CTL expansion and function were assessed at day 8 following infection. Gp33-specific CTL expanded to comparable numbers in C57BL/6 mice, T-LT β ^{-/-} mice

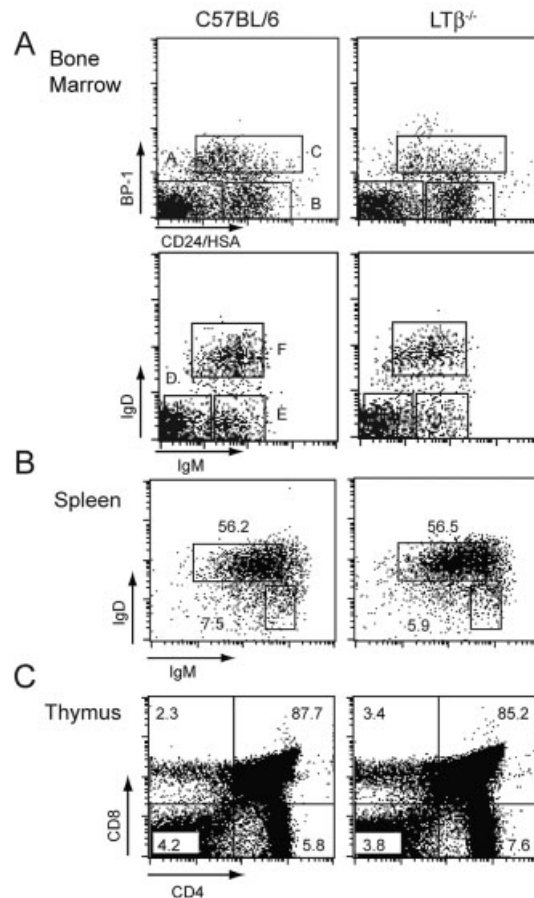


Fig. 6. No detectable difference in the frequency of immature T cell and B cells between C57BL/6 and LT β ^{-/-} mice. (A, upper) BP-1 and CD24/HSA expression on bone marrow cells of C57BL/6 and LT β ^{-/-} mice; dot plots were gated on B220⁺/CD43⁺ cells. Frequencies for C57BL/6: Fr.A: 48.2 ± 12%, Fr.B: 24.3 ± 4.8%, Fr.C: 13.3 ± 5.2%, for LT β ^{-/-}: Fr.A: 51.4 ± 7.6%, Fr.B: 22.0 ± 4.8%, Fr.C: 11.8 ± 2.6% (n = 3–8). (A, lower). IgM and IgD expression on bone marrow cells of C57BL/6 and LT β ^{-/-} mice; dot plots were gated on B220⁺/CD43⁻ cells. Frequencies for C57BL/6: Fr.D: 42.9 ± 2.2%, Fr.E: 15.3 ± 0.4%, Fr.F: 17.3 ± 2.0%, for LT β ^{-/-}: Fr.D: 46.2 ± 1.6%, Fr.E: 13.1 ± 3.2%, Fr.F: 25.2 ± 3.8% (n = 3–8, ± SD). (B) Frequencies of IgM^{high}/IgD^{low} transitional and IgM^{int}/IgD^{high} mature B cells in spleens of LT β ^{-/-} and C57BL/6 mice. Dot plots were gated on B220⁺ lymphocytes. (C) CD4 and CD8 expression of thymocytes of C57BL/6 and LT β ^{-/-} mice, gated on live lymphocytes. Mean percentages are shown for (B) and (C) and are representative of two to three similar experiments.

and B-LT $\beta^{-/-}$ mice, within the spleen, MLN and blood, as shown by LCMV-gp33-specific tetramer analysis. However, TB-LT $\beta^{-/-}$ and particularly LT $\beta^{-/-}$ showed reduced numbers of gp33-specific CTL in the spleen (Fig. 8A). Peptide-specific IFN- γ production following *in vitro* restimulation for 6 h was detected in spleens and MLN of all mice except LT $\beta^{-/-}$, with a small reduction of the frequency of IFN- γ -producers in T-LT $\beta^{-/-}$ mice, a more substantial reduction in B-LT $\beta^{-/-}$ and TB-LT $\beta^{-/-}$ mice, and an almost complete absence of gp33-specific IFN- γ production in LT $\beta^{-/-}$ mice (Fig. 8B). Similarly, all LT β -deficient mouse strains were impaired in their capacity to specifically lyse ^{51}Cr -labeled target cells (Fig. 8C, left

and middle panels). The impairment of CTL induction correlated well with the increasing disorganization of lymphoid structure in the various LT β -deficient mice. Completely LT β -deficient mice did not mount a measurable specific CTL response, even following secondary restimulation *in vitro* on gp33-pulsed macrophages (Fig. 8C, right panel). The observed phenotypes for CTL activation and expansion were mirrored by antiviral protection (Fig. 5D): C56BL/6, T-LT $\beta^{-/-}$ and B-LT $\beta^{-/-}$ had completely cleared LCMV from spleen, liver and kidney by day 8 post infection. TB-LT $\beta^{-/-}$ but not LT $\beta^{-/-}$ mice had eliminated the virus by day 30 post infection (data not shown), consistent with a previous

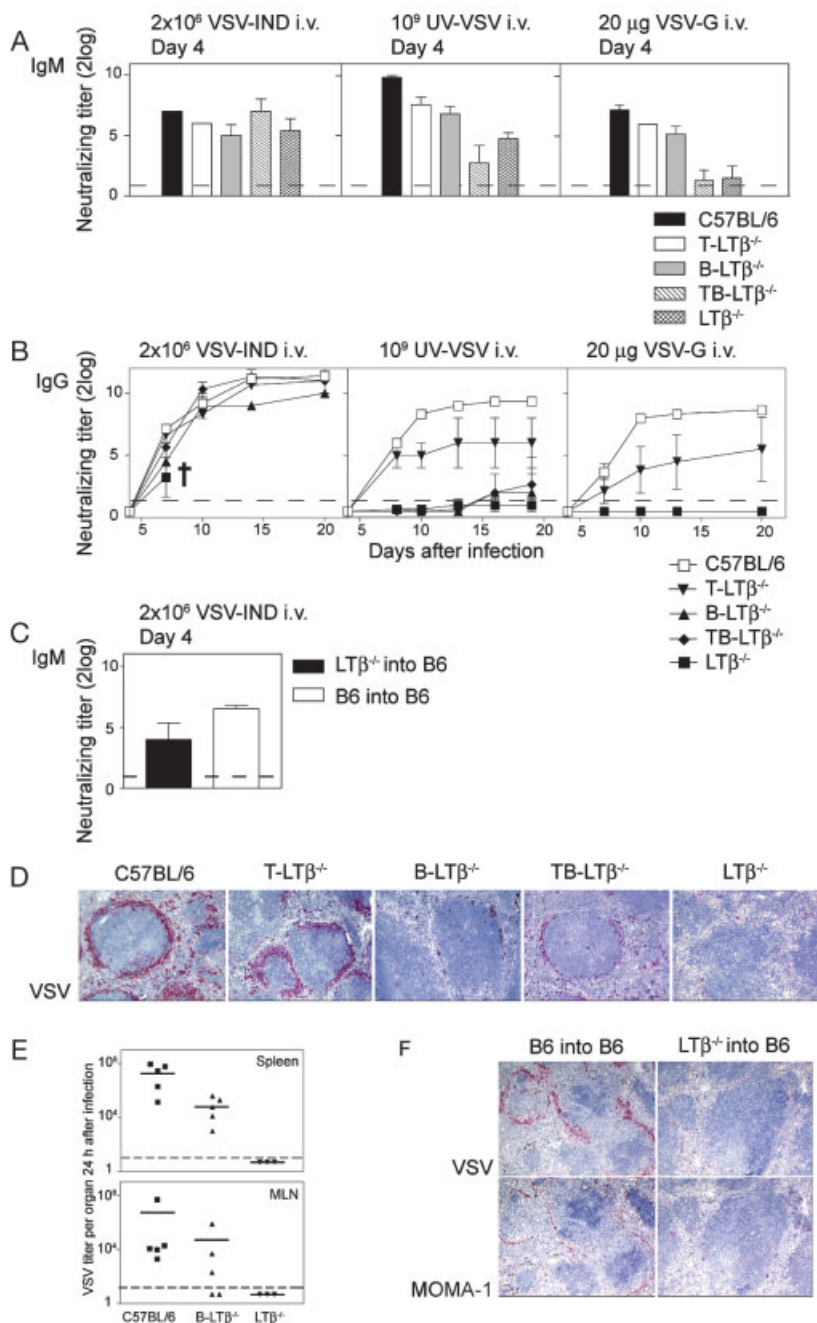


Fig. 7. Normal immune responses to VSV in conditional LT β -knockout mouse strains, versus impaired immune responses to UV-VSV and VSV-G. (A) IgM responses to replicating and non-replicating viral antigens. Antibody titers of LT-deficient mice and C57BL/6 mice were determined in mice immunized *i.v.* with 2×10^6 PFU VSV-IND (left panel), 10^9 PFU UV-VSV (center panel) or $20 \mu\text{g}$ VSV-G (right panel) on day 4 following immunization. Bars represent mean values \pm SD of $n = 3$ –6 mice. (B) IgG production of LT β -deficient mouse strains following immunization with 2×10^6 PFU VSV-IND (left panel), 10^9 PFU UV-VSV (center panel) or $20 \mu\text{g}$ VSV-G (right panel). Data points represent means \pm SD of $n = 3$ –6 mice. (C) IgM production of B6 \rightarrow B6 and LT β \rightarrow B6 bone marrow chimeras on day 4 following infection with 2×10^6 PFU VSV-IND, $n = 3$, \pm SD; (D) Capture of viral antigen in the spleen 24 h following infection with 5×10^8 PFU (original magnification: 120x). Note that localization and intensity of VSV staining correlates to the staining of MOMA-1 (see Fig. 1A). (E) VSV titers in spleens (top panel) and MLN (bottom panel) 24 h after infection with 5×10^8 PFU VSV-IND *i.v.*, horizontal bar represents means. (F) Capture of viral antigen in the spleen of B6 \rightarrow B6 and LT β \rightarrow B6 bone marrow chimeras 24 h after infection with 5×10^8 PFU VSV-IND.

report showing that $LT\beta^{-/-}$ mice have the propensity to become virus carriers [16].

Antiviral CTL can be induced by antigen presentation in the MZ or T cell zone of the spleen [18]. B- $LT\beta^{-/-}$ and $LT\beta^{-/-}$ mice exhibited fewer LCMV-infected cells at these sites (Fig. 9, upper panel). When the LCMV-infected cells were further analyzed, we found similar overall

frequencies of infected cells in spleens (Fig. 9B, red numbers), but the types of infected cells were distinct (Fig. 9B): In C57BL/6 mice a significant proportion of infected cells were DC. Declining numbers of LCMV-infected DC were detected in B- $LT\beta^{-/-}$ mice that exhibited weaker specific CTL responses, and in $LT\beta^{-/-}$ mice, where no CTL priming was observed. A

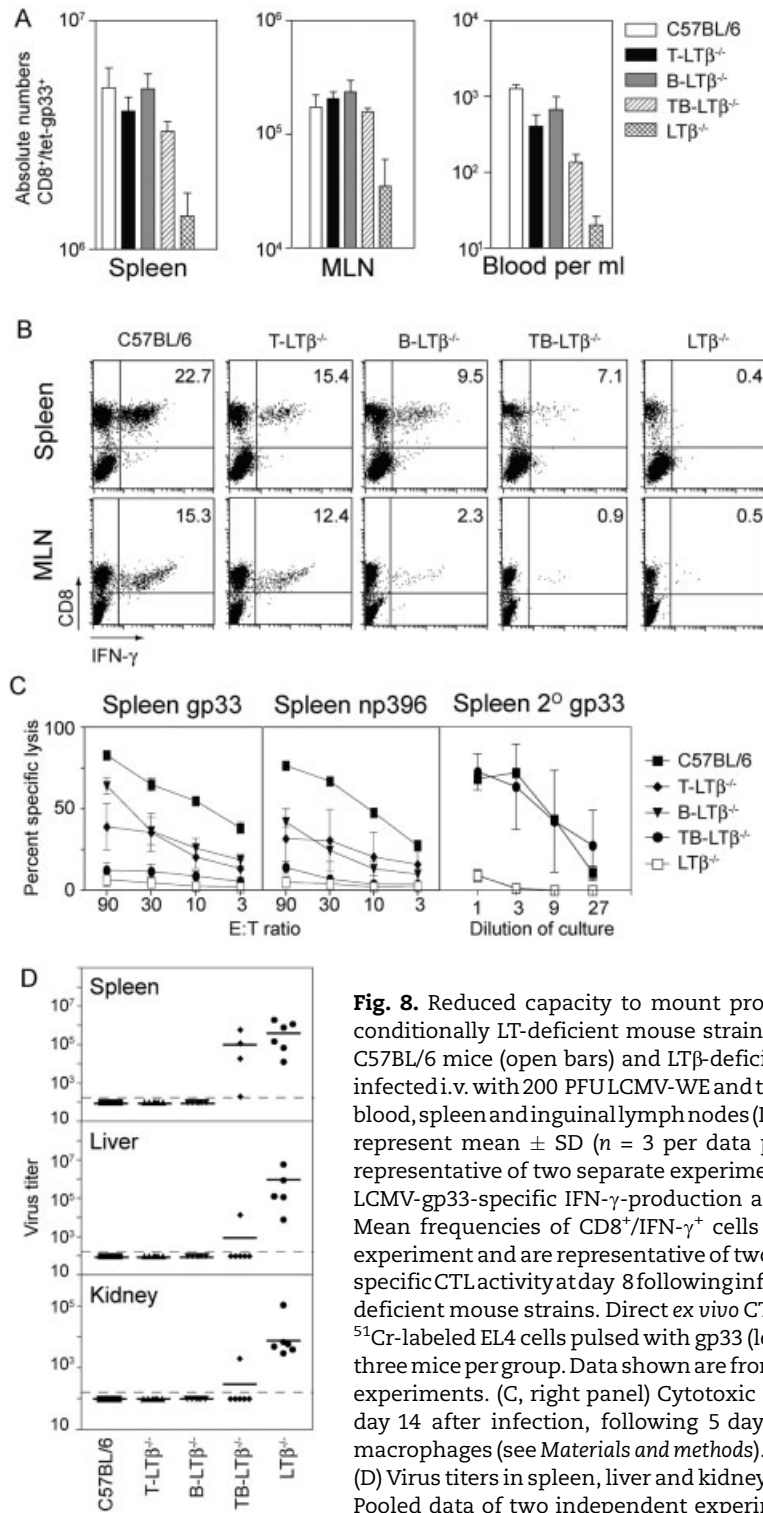


Fig. 8. Reduced capacity to mount productive CTL responses but full antiviral protection in conditionally LT-deficient mouse strains. (A) Expansion of LCMV-gp33-specific CD8⁺ T cells in C57BL/6 mice (open bars) and LT β -deficient mouse strains (filled and hatched bars). Mice were infected i.v. with 200 PFU LCMV-WE and total cell numbers of CD8⁺tet-gp33⁺ CTL were assessed for blood, spleen and inguinal lymph nodes (ILN) on day 8 postinfection by FACS analysis. Given values represent mean \pm SD ($n = 3$ per data point). Data shown are from one experiment and are representative of two separate experiments. (B) Spleens of the indicated mice were analyzed for LCMV-gp33-specific IFN- γ -production at day 8 following infection with 200 PFU LCMV-WE i.v. Mean frequencies of CD8⁺/IFN- γ ⁺ cells are indicated ($n = 3$ mice). Data shown are from one experiment and are representative of two separate experiments. (C, left and middle panel) LCMV-specific CTL activity at day 8 following infection with 200 PFU LCMV-WE i.v. in C57BL/6 mice and LT-deficient mouse strains. Direct *ex vivo* CTL activity of spleen and lymph node cells was tested on ⁵¹Cr-labeled EL4 cells pulsed with gp33 (left) or np396 (middle). Data points indicate mean \pm SD of three mice per group. Data shown are from one experiment and are representative of two separate experiments. (C, right panel) Cytotoxic activity of C57BL/6, TB- $LT\beta^{-/-}$ and $LT\beta^{-/-}$ splenocytes on day 14 after infection, following 5 days of secondary *in vitro* restimulation on gp33-pulsed macrophages (see *Materials and methods*). Data points indicate mean \pm SD of three mice per group. (D) Virus titers in spleen, liver and kidney on day 8 following infection with 200 PFU LCMV-WE i.v. Pooled data of two independent experiments are shown, horizontal bar represents means.

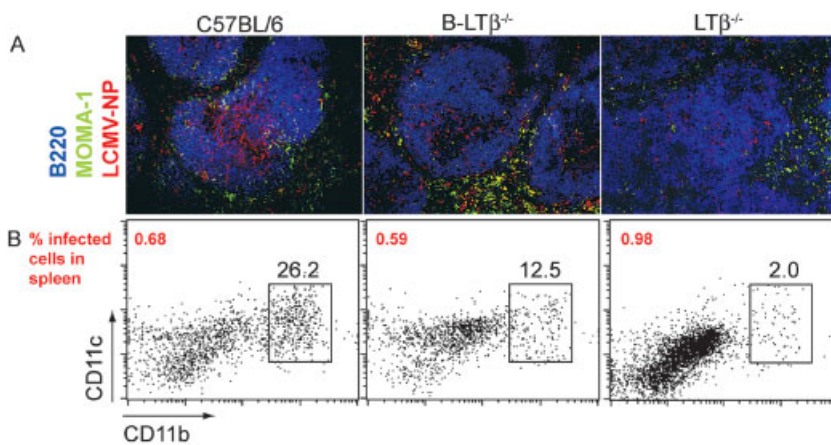


Fig. 9. Characterization of LCMV-infected DC in spleens on day 2 following infection with LCMV-WE. (A) Primary site of LCMV infection in the spleen on day 2 following infection of C57BL/6, B-LTβ^{-/-} and LTβ^{-/-} mice with 2×10^6 PFU LCMV-WE i.v. LCMV-NP (VL-4)-positive cells in spleens are indicated in red. Original magnification is 120x. (B) Red numbers indicate the percentages of splenocytes staining positive for LCMV-NP, and are means of $n = 2$ –5 mice. Dot plots are gated on LCMV-NP (VL-4)-positive splenocytes, and black numbers represent percentages of CD11c⁺/CD11b⁺ cells in this population. Data are from one representative of $n = 2$ –5 mice.

high number of LCMV-infected DC in the spleen thus correlated with a strong antiviral CTL response and with antiviral protection (see Fig. 8). LCMV replicated inefficiently in splenic DC of LTβ^{-/-} mice, likely causing inefficient CTL priming, uncontrolled virus spread and CTL exhaustion.

In line with recent findings that DC are critical for the LCMV-specific CTL response [31], we thus propose that the LTβ-dependent integrity of DC networks is key for the outcome of the virus-specific CTL response.

Discussion

In this study, we have made use of two well-established virus models, the non-cytopathic LCMV and the cytopathic VSV to study the relevance of LTβ-dependent lymphoid structure for initial containment of an infection and the induction of T and B cell responses. The failure to contain a cytopathic virus such as VSV resulted in death of the host, and the failure to rapidly contain an infection with a non-cytopathic virus such as LCMV resulted in virus persistence.

The formation of secondary lymphoid organ structure by LTβ-dependent mechanisms is crucial for the induction of immune responses against viruses [16] and proteins [21], but it is not clear, at which level LTβ regulates the immune response. We have shown here that absence of LTβ does not interfere with lymphocyte development or activation on the single-cell level. Therefore, LTβ is likely to determine immune reactivity mainly *via* its impact on lymphoid structure. LTβ regulates lymphoid structure at two levels: LTβ on LTIC is critical for the commitment of secondary lymphoid

organ anlage sites [2], LTβ expression on B cells, T cells, LTIC, and potentially other cells such as NK cells defines lymphoid structure *via* the induction of chemokines [21, 32, 33]. The generation of conditionally LTβ-deficient mice has allowed us to dissect the relevance of these two levels of LTβ-dependent organization during immune responses.

The series of C57BL/6, T-, B-, and TB-LTβ^{-/-} mice was found to reflect a gradual decline of LTβ-dependent secondary lymphoid structure. Interestingly, conditional LTβ deficiency caused a more pronounced structural defect in spleens than in lymph nodes, and the morphological alterations in B-LTβ^{-/-} mice were more severe than in T-LTβ^{-/-} mice, despite similar expression levels of LTβ in spleens and lymph nodes. This was either caused by the fact that B cells represent the prime source for LTβ during secondary lymphoid organ development [34], or because the microstructures of lymph nodes *versus* spleen rely to a different extent on LTβ expression [13]. Surprisingly, we did not find a gradual decline of B cell reactivity in T-, B-, and TB-LTβ^{-/-} mice. Instead, normal titers of neutralizing IgM and IgG were raised against VSV infection in all strains. In contrast, the non-replicating antigens UV-VSV and VSV-G both elicited reduced titers of IgM and IgG in all conditionally LTβ-deficient mice, irrespective of the degree of lymphoid organ malformation. Reduced formation of IgG has also been observed in B-LTβ^{-/-} and LTβ^{-/-} mice when another non-replicating antigen, SRBC, was used as an antigen [21]. The stepwise impairment of lymphoid structure therefore did not necessarily play a role for the vigor of a B cell response. However, the maturation of the virus-neutralizing B cell response may have been affected in LTβ-deficient mice, because the GC that were

induced did not contain FDC-M1⁺ networks in some LTβ-deficient strains. In addition, lymphoid structure did not affect the protective capacity of an antiviral CTL response, but rather the magnitude of this response, as all conditionally LTβ-deficient mouse strains were protected against LCMV, but the clonal burst was somewhat weaker in T- and B-LTβ^{-/-} mice, and protection was slower in TB-LTβ^{-/-} mice. The deficiency of NK cells in LTβ^{-/-} mice [22] may additionally negatively affect early VSV control [35, 36], but there is evidence that the absence of NK cells does not significantly delay LCMV clearance [37].

The role of LTβ in lymph node anlage commitment became apparent if TB-LTβ^{-/-} mice were compared with LTβ^{-/-} mice. Commitment of anlage sites was governed by expression of LTβ on non-T/non-B cells, because TB-LTβ^{-/-} mice had all lymph nodes with normal cellularity. Similarly, these cells are responsible for the induction of a functional MZ, and the accumulation of MOMA-1⁺ macrophages in the marginal sinus in TB-LTβ^{-/-} mice. Bone marrow reconstitutions of LTβ^{-/-}→B6 established that it was not the reduced number of lymph nodes, but the complete absence of a functional MZ that caused death of LTβ^{-/-} mice following VSV infection.

An intact MZ also contributes to the initial containment of LCMV infection, preventing hematogenic spread and excessive replication of the virus in the periphery [30, 38]. Therefore, the reduced CTL priming efficiency in B-LTβ^{-/-}, TB-LTβ^{-/-} and LTβ^{-/-} could partly be caused by a defective MZ. CTL priming efficiency additionally correlated with a high number of LCMV-infected DC, in line with the key role of DC in antiviral protection against LCMV [31].

Overall, we conclude that the expression of LTβ by T or B lymphocytes creates specialized environments for the detection of low quantities of antigen (e.g. UV-VSV, VSV-G, and SRBC) by rare precursor cells. However, these LTβ-dependent lymphoid microenvironments seemed of minor importance if large quantities of antigen (e.g. replicating virus) efficiently reached secondary lymphoid organs. Expression of LTβ on non-T, non-B cells (i.e. NK cells, macrophages or LTIC) was responsible for the induction of macrophage networks at the MZ and for the generation of DC networks. If these organized sites of antigen presentation were missing, antigen could not be efficiently retained and presented within secondary lymphoid organs. Consequently, virus spread systemically and no efficient immune response was induced. This eventually resulted in CTL exhaustion following LCMV infection, or death of the host following VSV infection. LTβ expression thus influences immunity at two distinct levels: (i) by increasing the probability of cell-cell interactions within secondary lymphoid organs, and (ii) by supporting antigen sampling of APC within secondary lymphoid organs.

The fact that even minor alterations of secondary lymphoid organ microstructure impaired immune responses against non-replicating antigens underscores the importance of lymphoid microstructure for vaccinations. Vaccinations are most frequently performed with attenuated or inactivated pathogens, with proteins or with low amounts of other non-replicating antigens. In humans, there is one particular and crucial situation where a defective lymphoid structure can limit the efficacy of vaccinations. Newborns lack clearly organized lymphoid structures [39]; in particular, they exhibit an immature MZ [40]. This may explain why newborns fail to induce potent immune responses against many vaccines [41].

Materials and methods

Mice

LTβ-floxed mice [21] were crossed to CD19Cre knock-in mice [42] or to the lckCre transgenic mice [43] for subsequent generation of B-LTβ^{-/-} and T-LTβ^{-/-} mice, respectively. The lckCre and CD19Cre constructs ablated expression of LTβ on T and B cells, respectively, to more than 98% [13]. T-LTβ^{-/-} mice and B-LTβ^{-/-} mice were intercrossed to obtain TB-LTβ^{-/-} mice. LTβ^{-/-} mice were bred and genotyped as described [8]. The following PCR conditions were chosen for typing of the LTβ-flox allele: Pri3ltb: 5'-GGG AGG GGAT TG TGT CCG AG-3'; Pri5ltb: 5'-TCT TCC CTA AAC TCC AAT CAG C-3'; KO46: 5'-GGG GTG ACC TAG ATA GTG CC-3'; 35 cycles of 94°C, 45 s; 61°C, 45 s; 72°C, 60 s (products for WT: 0.2 kb, LTβ-flox: 0.25 kb, deleted 0.4 kb). For typing of the CD19Cre allele: CD19.8: 5'-AAT GTT GTG CTG CCA TGC CTC-3'; CD19.9: 5'-GTC TGA AGC ATT CCA CCG GAA-3'; lck2: 5'-AAT GTT GCT GGA TAG TTT TTA CTG C-3'; 35 cycles of 94°C, 60 s; 60°C, 60 s 72°C, 120 s (products for WT: 500 bp, for CD19Cre: 400 bp). For typing of the lckCre allele: lck1: 5'-CCT TGG TGG AGG AGG GTG GAA TGA A-3'; lck2: 5'-AAT GTT GCT GGA TAG TTT TTA CTG C-3'; lck3: 5'-TAG AGC CCT GTT CTG GAA GTT ACA A-3'; 35 cycles of 94°C, 60 s; 60°C, 60 s 72°C, 120 s (products for WT: 0.35 kb, for lckCre 0.6 kb). All mice were backcrossed to C57BL/6 for at least nine times. BM chimeras were generated by lethal irradiation (9.5 Gy from a ⁵⁷Co source) of C57BL/6 mice and i.v. injection of BM cells from sex-matched donors. BM chimeras were given Borgal (Hoechst Roussel Vet, Lyssach, Switzerland) in the drinking water (1 mg/mL Sulfadoxin, 0.2 mg/mL Trimethoprim) during the first 2 weeks after reconstitution and left for 8 weeks before use in experiments. Animals were kept at the Biologische Zentrallabor, University of Zürich, Switzerland. All animal experiments were performed in accordance with the Swiss Federal legislation on animal protection.

Viruses and peptides

LCMV, WE strain, originally obtained from Dr. F. Lehmann-Grube (Heinrich-Pette-Institut, Hamburg, Germany), was propagated on L929 cells at a low MOI and was quantified

as previously described [44]. VSV, Indiana strain (VSV-IND, Mudd-Summers isolate), was originally obtained from Prof. D. Kolakofsky (University of Geneva, Switzerland). VSV-IND was propagated on baby hamster kidney 21 (BHK-21) cells and quantified by plaque assay on Vero cells. For some experiments, UV-inactivated VSV-IND was obtained using UV irradiation (7UV 15 W, Philips) for 3 min using a thin layer of solution in a plastic dish with periodical mixing. The LCMV-GP peptide KAVYNFATC (gp33) and the LCMV-NP peptide FQPGNGQFI (np396) were purchased from Neosystem (Strasbourg, France).

LCMV-specific cytotoxic T cell response

Specific cytotoxicity was determined *ex vivo* in a standard ^{51}Cr -release assay as described [45]. Briefly, cell suspensions were prepared from spleens or lymph nodes of immunized mice at the indicated time point after priming. For LCMV-specific CTL assays, EL-4 cells were labeled with gp33 (10^{-6} M) and 250 μCi ^{51}Cr for 1.5 h at 37°C. Target cells (10^4 /well) were incubated for 4 h in 96-well round-bottom plates with threefold serial dilutions of spleen or lymph node effector cells, starting at an effector to target (E:T) ratio of 90:1. EL-4 cells without peptide served as controls. The supernatants of the cytotoxicity assay cultures were counted in a Cobra II Gamma Counter (Canberra Packard). Percentage of specific lysis was calculated as (experimental release – spontaneous release)/(total release – spontaneous release) \times 100. Spontaneous release was always below 20%. In some experiments, the ^{51}Cr -release assay followed a 5-day restimulation period of splenocytes on irradiated thioglycollate-elicited peritoneal macrophages pulsed with gp33.

VSV neutralization assay

Neutralizing antibody titers of sera were determined as described [46]. Sera were prediluted 40-fold in supplemented MEM and heat-inactivated for 30 min at 56°C. Serial 2-fold dilutions were mixed with equal volumes of virus diluted to contain 500 PFU/mL. The mixture was incubated for 90 min at 37°C in an atmosphere containing 5% CO_2 . The serum-virus mixture (100 μL) was transferred onto Vero cell monolayers in 96-well plates and incubated for 1 h at 37°C. The monolayers were then overlaid with 100 μL DMEM containing 1% methyl cellulose. After incubation for 24 h at 37°C the overlay was removed and the monolayer was fixed and stained with 0.5% crystal violet. The highest dilution of the serum that reduced the number of plaques by 50% was taken as the neutralizing titer. IgG titers were determined by treating undiluted serum with an equal volume of 0.1 M 2-ME in saline.

Construction of tetrameric class I-peptide complexes and flow cytometry

All fluorochrome-labeled antibodies for cytofluorimetric analyses and for fluorescence microscopy were purchased from PharMingen BD unless indicated otherwise. MHC class I (H-2D^b) tetramers complexed with gp33 were produced as previously described [47] with modifications [48]. At the indicated time points after immunization, animals were bled

and single-cell suspensions were prepared from spleen and lymph nodes. Aliquots of 5×10^5 cells or three drops of blood were stained using 50 μL of a solution containing tetrameric class I-peptide complexes at 37°C for 10 min followed by staining with anti-CD8-FITC (BD PharMingen) at 4°C for 20 min. Erythrocytes in blood samples were lysed with FACS lysis solution (Becton Dickinson) and the cells were analyzed on a FACScalibur flow cytometer (Becton Dickinson) after gating on viable leukocytes, using the Cellquest software. For the determination of absolute cell counts, the number of total viable leukocytes was assessed in an improved Neubauer chamber. The number of total viable leukocytes in blood was automatically determined in an Advia counter (Bayer, Germany) in the Central Hematology Laboratory of the University Hospital Zürich.

Intracellular cytokine staining

Spleens were removed at the indicated time points after infection with LCMV. Single-cell preparations of 1×10^6 splenocytes were incubated for 5 h at 37°C in 96-well round-bottom plates in 200 μL culture medium containing 25 U/mL IL-2 and 5 $\mu\text{g}/\text{mL}$ Brefeldin A (Sigma). Splenocytes were stimulated with PMA (50 ng/mL) and ionomycin (500 ng/mL) as a positive control or left untreated as a negative control. For analysis of peptide-specific responses, 10^6 splenocytes were stimulated by adding 10^{-6} M gp33. After stimulation, splenocytes were surface stained with anti-CD8-PE (53–5.8, PharMingen) in FACS-buffer (PBS + 2% FCS + 20 mM EDTA + 0.03% NaN_3) for 1 h at 4°C. Splenocytes were washed once with FACS-buffer, fixed with 100 μL 4% paraformaldehyde in PBS for 5 min at 4°C, and permeabilized with 2 mL of permeabilization buffer (FACS-buffer + 0.1% saponin) for 5 min at 4°C. Cells were then stained intracellularly with anti-IFN- γ -FITC (AN18, [49]) in permeabilization buffer for 30 min at 4°C. Cells were washed twice with permeabilization buffer, and the percentage of IFN- γ -producing cells was determined after gating on CD8⁺ cells using a FACScalibur flow cytometer. Data analysis was performed with the Cellquest software.

Homing experiments

Thy1.2⁺ T cells and B220⁺ B cells were purified by magnetic-bead assisted cell sorting (MACS, Miltenyi Biotech, Bergisch Gladbach, Germany) from spleens of C57BL/6 mice or $\text{LT}\beta^{-/-}$ mice and labeled with CFSE for 10 min at 37°C as described [50]. Cells (3×10^6) were adoptively transferred *i.v.* to naive C57BL/6 mice. Six hours post transfer, spleens were taken and analyzed by fluorescence microscopy.

Immunohistochemistry and fluorescence microscopy

For immunohistochemistry, 5- μm cryostat sections were fixed in acetone for 10 min and subsequently incubated with anti-mouse B220 (RA3–3A1/6.1, ATCC, Rockville, MD), anti-mouse CD4 (GK1.5), anti-mouse CD8 (53–6.7, BD PharMingen), anti-mouse 4C11 (FDCM1, BD Biosciences), anti-mouse MadCAM (MECA367, PharMingen) or anti-mouse MOMA-1 [51]. Goat anti-rat Ig (Caltag) in 5% normal mouse serum was used as a secondary reagent, alkaline phosphatase-labeled,

species-specific donkey anti-goat (Jackson ImmunoResearch) in 5% normal mouse serum was used as tertiary reagents. The substrate for the red color reaction was naphthol AS-BI phosphate/New Fuchsin. Endogenous alkaline phosphatase was blocked with levamisole. Sections were counterstained with hemalum. Staining for VSV antigen was performed as described previously [52]. For fluorescence microscopy, acetone-fixed 5- μ m cryostat sections were incubated for 10 min with 10 μ g/mL 2.4G2 antibody to block Fc receptors, and washed with PBS. Sections were then incubated for 60 min with 10 μ g/mL of the biotinylated or FITC-labeled antibodies in a wet chamber, washed with PBS, and incubated with streptavidin-TRITC for 30 min in a wet chamber. Sections were washed in PBS, counterstained with DAPI (Chemicon International, Temecula, CA), mounted with fluorescence mounting solution (DAKO, Carpinteria, CA) and analyzed by fluorescence microscopy using a BX61 fluorescence microscope (Olympus, Volketswil, Switzerland). All reagents for fluorescent microscopy were diluted in PBS 1%FCS.

In vitro restimulation of T and B cells and ELISA

CD4⁺ and CD8⁺ T cells were isolated from splenocyte suspensions of C57BL/6 mice or LT β ^{-/-} mice by MACS (Miltenyi Biotech, Bergisch Gladbach, Germany). They were cultivated in RPMI 10% FCS for 3 or 5 days on plastic plates coated with 10 μ g/mL anti-CD3 (2C11) in the presence of 10 mg/mL anti-CD28 (37.51) and 50 U/mL IL-2. Untouched B cells were isolated from splenocyte suspensions of C57BL/6 mice and LT β ^{-/-} mice by MACS using anti-CD43 magnetic beads and an AutoMACS separator. They were cultivated in RPMI 10% FCS for 3 days in the presence of 15 μ g/mL anti-CD40 (FGK45.5, a kind gift from A. Rolink) and 1000 U/mL recombinant mouse IL-4 or 500 U/mL recombinant mouse IFN- γ , respectively. In some cases, anti-CD40 was replaced by 10 μ g/mL LPS. In some experiments, cells were labeled with CFSE as described [50].

Real-time PCR

RNA was extracted using TRIZOL according to manufacturer's instructions (Invitrogen). Extracted RNA (2 μ g) was subjected to DNase digest and subsequent reverse transcription using the Superscript kit (Invitrogen). SYBRgreen-based (Applied Biosystems, Foster City, CA) real-time PCR was carried out in an ABIPrism 7700 Sequence Detector using the SDS 1.9 software and the following primers: LT β .up: 5'- CGT CTA TTA CCT CTA CTG CC -3'; LT β .do: 5'- CGT GTA CCA TAA CGA CCC GT -3'; LT α .up: 5'- CCC TCA GAA GCA CTT GAC C -3'; LT α .do: 5'- CAG AGA AAA CCA CCT GGG AG -3'; TNF.up: 5'- CAT CTT CTC AAA ATT CGA GTG ACA A -3'; TNF.do: 5'- TGG GAG TAG ACA AGG TAC AAC CC -3'; LIGHT.up: 5'- ATG GAG AGT GTG GTA CAG CCT TC -3'; LIGHT.do: 5'- GAC CAT GAA AGC TCC GAA ATA GG -3'; GAPDH.up: 5'- CCA CCC CAG CAA GGA CAC T -3'; GAPDH.do: 5'- GAA ATT GTG AGG GAG ATG CTC AGT -3'. Cell populations were MACS-sorted from spleens of naive B6 mice as follows: B cells, CD43 depletion; T cells, CD4 or CD8 enrichment; NK cells, DX5 enrichment, DC, CD11c enrichment. Macrophages were isolated from peritoneal lavages by B220 and DX5 depletion and subsequent CD11b enrichment.

Purities ranged between 85% (NK cells) to >92% (all other cell types). Similar LT β expression data were obtained with FACS-sorted cells (FACSaria, BD Biosciences). Relative mRNA expression was calculated as follows: Δ ct values between the expression curves of LT β and GAPDH were determined for all samples. The mean Δ ct value for B6 samples was subtracted from all other samples to determine expression levels relative to B6. $\Delta\Delta$ ct values were then converted to percent by taking into account the PCR amplification factor 2^x, and SD were calculated within each experimental group.

Acknowledgements: This study was funded by grants of the Swiss National Science Foundation and the Kanton of Zürich, by MCB grants from the Russian Academy of Sciences, the Russian Foundation of Basic Research. M.H. was supported by the foundation for research at the Medical Faculty, University of Zürich, a generous educational grant of the Catello family, and a grant of the Verein zur Förderung des Akademischen Nachwuchses. S.A.N. is an international Scholar of the Howard Hughes Medical Institute. We are grateful to Antje Nowotny and Silvia Behnke for immunohistochemistry and to Drs. Maries van den Broek and Sanjiv Luther for valuable discussions. In addition, we thank Sergei Grivennikov and Anna Khalatova for help with mouse genotyping, Lars Hangartner for the VL-4 antibody, and Kathrin Tschannen for generation of gp33-tetramers. In addition, we want to thank the personnel of Laboratory Animal Breeding Center, Branch of Schemyakin and Ovchinnikov Institute of Bioorganic Chemistry for expert help with mouse breeding and production.

References

- 1 Fu, Y. X. and Chaplin, D. D., Development and maturation of secondary lymphoid tissues. *Annu. Rev. Immunol.* 1999. **17**: 399–433.
- 2 Finke, D., Acha-Orbea, H., Mattis, A., Lipp, M. and Kraehenbuhl, J., CD4⁺CD3⁻ cells induce Peyer's patch development: role of alpha4beta1 integrin activation by CXCR5. *Immunity* 2002. **17**: 363–373.
- 3 Mebius, R. E., Rennert, P. and Weissman, I. L., Developing lymph nodes collect CD4⁺CD3⁻LTbeta⁺ cells that can differentiate to APC, NK cells, and follicular cells but not T or B cells. *Immunity* 1997. **7**: 493–504.
- 4 Nishikawa, S., Honda, K., Vieira, P. and Yoshida, H., Organogenesis of peripheral lymphoid organs. *Immuno. Rev.* 2003. **195**: 72–80.
- 5 Ngo, V. N., Korner, H., Gunn, M. D., Schmidt, K. N., Riminton, D. S., Cooper, M. D., Browning, J. L. et al., Lymphotoxin alpha/beta and tumor necrosis factor are required for stromal cell expression of homing chemokines in B and T cell areas of the spleen. *J. Exp. Med.* 1999. **189**: 403–412.
- 6 De Togni, P., Goellner, J., Ruddle, N. H., Streeter, P. R., Fick, A., Mariathasan, S., Smith, S. C. et al., Abnormal development of peripheral lymphoid organs in mice deficient in lymphotoxin. *Science* 1994. **264**: 703–707.
- 7 Banks, T. A., Rouse, B. T., Kerley, M. K., Blair, P. J., Godfrey, V. L., Kuklin, N. A., Bouley, D. M. et al., Lymphotoxin-alpha-deficient mice. Effects on secondary lymphoid organ development and humoral immune responsiveness. *J. Immunol.* 1995. **155**: 1685–1693.
- 8 Alimzhanov, M. B., Kuprash, D. V., Kosco-Vilbois, M. H., Luz, A., Turetskaya, R. L., Tarakhovskiy, A., Rajewsky, K. et al., Abnormal

- development of secondary lymphoid tissues in lymphotoxin beta-deficient mice. *Proc. Natl. Acad. Sci. USA* 1997. **94**: 9302–9307.
- 9 Koni, P. A., Sacca, R., Lawton, P., Browning, J. L., Ruddle, N. H. and Flavell, R. A., Distinct roles in lymphoid organogenesis for lymphotoxins alpha and beta revealed in lymphotoxin beta-deficient mice. *Immunity* 1997. **6**: 491–500.
 - 10 Futterer, A., Mink, K., Luz, A., Kosco-Vilbois, M. H. and Pfeffer, K., The lymphotoxin beta receptor controls organogenesis and affinity maturation in peripheral lymphoid tissues. *Immunity* 1998. **9**: 59–70.
 - 11 Honda, K., Nakano, H., Yoshida, H., Nishikawa, S., Rennert, P., Ikuta, K., Tamechika, M. et al., Molecular basis for hematopoietic/mesenchymal interaction during initiation of Peyer's patch organogenesis. *J. Exp. Med.* 2001. **193**: 621–630.
 - 12 Ansel, K. M., Ngo, V. N., Hyman, P. L., Luther, S. A., Forster, R., Sedgwick, J. D., Browning, J. L. et al., A chemokine-driven positive feedback loop organizes lymphoid follicles. *Nature* 2000. **406**: 309–314.
 - 13 Tumanov, A. V., Grivennikov, S. I., Shakhov, A. N., Rybtsov, S. A., Koroleva, E. P., Takeda, J., Nedospasov, S. A. and Kuprash, D. V., Dissecting the role of lymphotoxin in lymphoid organs by conditional targeting. *Immunol. Rev.* 2003. **195**: 106–116.
 - 14 Campbell, D. J., Kim, C. H. and Butcher, E. C., Chemokines in the systemic organization of immunity. *Immunol. Rev.* 2003. **195**: 58–71.
 - 15 Suresh, M., Lanier, G., Large, M. K., Whitmire, J. K., Altman, J. D., Ruddle, N. H. and Ahmed, R., Role of lymphotoxin alpha in T-cell responses during an acute viral infection. *J. Virol.* 2002. **76**: 3943–3951.
 - 16 Berger, D. P., Nanche, D., Crowley, M. T., Koni, P. A., Flavell, R. A. and Oldstone, M. B., Lymphotoxin-beta-deficient mice show defective antiviral immunity. *Virology* 1999. **260**: 136–147.
 - 17 Lin, X., Ma, X., Rodriguez, M., Feng, X., Zoecklein, L., Fu, Y. X. and Roos, R. P., Membrane lymphotoxin is required for resistance to Theiler's virus infection. *Int. Immunol.* 2003. **15**: 955–962.
 - 18 Junt, T., Nakano, H., Dumrese, T., Kakiuchi, T., Odermatt, B., Zinkernagel, R. M., Hengartner, H. and Ludewig, B., Antiviral immune responses in the absence of organized lymphoid T cell zones in plt/plt mice. *J. Immunol.* 2002. **168**: 6032–6040.
 - 19 Junt, T., Scandella, E., Forster, R., Krebs, P., Krautwald, S., Lipp, M., Hengartner, H. and Ludewig, B., Impact of CCR7 on priming and distribution of antiviral effector and memory CTL. *J. Immunol.* 2004. **173**: 6684–6693.
 - 20 Junt, T., Fink, K., Forster, R., Senn, B., Lipp, M., Muramatsu, M., Zinkernagel, R. M. et al., CXCR5-dependent seeding of follicular niches by B and Th cells augments antiviral B cell responses. *J. Immunol.* 2005. **175**: 7109–7116.
 - 21 Tumanov, A., Kuprash, D., Lagarkova, M., Grivennikov, S., Abe, K., Shakhov, A., Drutskaya, L. et al., Distinct role of surface lymphotoxin expressed by B cells in the organization of secondary lymphoid tissues. *Immunity* 2002. **17**: 239–250.
 - 22 Wu, Q., Sun, Y., Wang, J., Lin, X., Wang, Y., Pegg, L. E., Futterer, A. et al., Signal via lymphotoxin-beta R on bone marrow stromal cells is required for an early checkpoint of NK cell development. *J. Immunol.* 2001. **166**: 1684–1689.
 - 23 Abe, K., Yarovinsky, F. O., Murakami, T., Shakhov, A. N., Tumanov, A. V., Ito, D., Drutskaya, L. N. et al., Distinct contributions of TNF and LT cytokines to the development of dendritic cells *in vitro* and their recruitment *in vivo*. *Blood* 2003. **101**: 1477–1483.
 - 24 Wu, Q., Wang, Y., Wang, J., Hedgeman, E. O., Browning, J. L. and Fu, Y. X., The requirement of membrane lymphotoxin for the presence of dendritic cells in lymphoid tissues. *J. Exp. Med.* 1999. **190**: 629–638.
 - 25 Boehm, T., Scheu, S., Pfeffer, K. and Bleul, C. C., Thymic medullary epithelial cell differentiation, thymocyte emigration, and the control of autoimmunity require lympho-epithelial cross talk via LTbetaR. *J. Exp. Med.* 2003. **198**: 757–769.
 - 26 Browning, J. L., Sizing, I. D., Lawton, P., Bourdon, P. R., Rennert, P. D., Majeau, G. R., Ambrose, C. M. et al., Characterization of lymphotoxin-alpha beta complexes on the surface of mouse lymphocytes. *J. Immunol.* 1997. **159**: 3288–3298.
 - 27 Millet, I. and Ruddle, N. H., Differential regulation of lymphotoxin (LT), lymphotoxin-beta (LT-beta), and TNF-alpha in murine T cell clones activated through the TCR. *J. Immunol.* 1994. **152**: 4336–4346.
 - 28 Li, Y. S., Wasserman, R., Hayakawa, K. and Hardy, R. R., Identification of the earliest B lineage stage in mouse bone marrow. *Immunity* 1996. **5**: 527–535.
 - 29 Ochsenbein, A. F., Fehr, T., Lutz, C., Suter, M., Brombacher, F., Hengartner, H. and Zinkernagel, R. M., Control of early viral and bacterial distribution and disease by natural antibodies. *Science* 1999. **286**: 2156–2159.
 - 30 Oehen, S., Odermatt, B., Karrer, U., Hengartner, H., Zinkernagel, R. and Lopez-Macias, C., Marginal zone macrophages and immune responses against viruses. *J. Immunol.* 2002. **169**: 1453–1458.
 - 31 Probst, H. C. and van den Broek, M., Priming of CTLs by lymphocytic choriomeningitis virus depends on dendritic cells. *J. Immunol.* 2005. **174**: 3920–3924.
 - 32 Ngo, V. N., Cornall, R. J. and Cyster, J. G., Splenic T zone development is B cell dependent. *J. Exp. Med.* 2001. **194**: 1649–1660.
 - 33 Cupedo, T. and Mebius, R. E., Cellular interactions in lymph node development. *J. Immunol.* 2005. **174**: 21–25.
 - 34 Ansel, K. M. and Cyster, J. G., Chemokines in lymphopoiesis and lymphoid organ development. *Curr. Opin. Immunol.* 2001. **13**: 172–179.
 - 35 Christian, A. Y., Barna, M., Bi, Z. and Reiss, C. S., Host immune response to vesicular stomatitis virus infection of the central nervous system in C57BL/6 mice. *Viral Immunol.* 1996. **9**: 195–205.
 - 36 Schattner, A. and Rager-Zisman, B., Lysis by natural killer cells requires viral replication and glycoprotein expression. *Immunol. Lett.* 1986. **13**: 261–268.
 - 37 Ehl, S., Nuesch, R., Tanaka, T., Myasaka, M., Hengartner, H. and Zinkernagel, R., A comparison of efficacy and specificity of three NK depleting antibodies. *J. Immunol. Methods* 1996. **199**: 149–153.
 - 38 Seiler, P., Aichele, P., Odermatt, B., Hengartner, H., Zinkernagel, R. M. and Schwendener, R. A., Crucial role of marginal zone macrophages and marginal zone metallophilic cells in the clearance of lymphocytic choriomeningitis virus infection. *Eur. J. Immunol.* 1997. **27**: 2626–2633.
 - 39 Timens, W., Rozeboom, T. and Poppema, S., Fetal and neonatal development of human spleen: an immunohistological study. *Immunology* 1987. **60**: 603–609.
 - 40 Timens, W., Boes, A., Rozeboom-Uiterwijk, T. and Poppema, S., Immaturity of the human splenic marginal zone in infancy. Possible contribution to the deficient infant immune response. *J. Immunol.* 1989. **143**: 3200–3206.
 - 41 Siegrist, C. A., Neonatal and early life vaccinology. *Vaccine* 2001. **19**: 3331–3346.
 - 42 Rickert, R. C., Roes, J. and Rajewsky, K., B lymphocyte-specific, Cre-mediated mutagenesis in mice. *Nucl. Acids Res.* 1997. **25**: 1317–1318.
 - 43 Takahama, Y., Ohishi, K., Tokoro, Y., Sugawara, T., Yoshimura, Y., Okabe, M., Kinoshita, T. and Takeda, J., Functional competence of T cells in the absence of glycosylphosphatidylinositol-anchored proteins caused by T cell-specific disruption of the Pig-a gene. *Eur. J. Immunol.* 1998. **28**: 2159–2166.
 - 44 Bategay, M., Cooper, S., Althage, A., Banziger, J., Hengartner, H. and Zinkernagel, R. M., Quantification of lymphocytic choriomeningitis virus with an immunological focus assay in 24- or 96-well plates [published errata appears in *J. Virol. Methods*. 1991 Nov;35(1):115 and 1992 Aug;38(2):263]. *J. Virol. Methods* 1991. **33**: 191–198.
 - 45 Hany, M., Oehen, S., Schulz, M., Hengartner, H., Mackett, M., Bishop, D. H., Overton, H. and Zinkernagel, R. M., Anti-viral protection and prevention of lymphocytic choriomeningitis or of the local footpad swelling reaction in mice by immunization with vaccinia-recombinant virus expressing LCMV-WE nucleoprotein or glycoprotein. *Eur. J. Immunol.* 1989. **19**: 417–424.
 - 46 Roost, H. P., Charan, S. and Zinkernagel, R. M., Analysis of the kinetics of antiviral memory T help *in vivo*: characterization of short-lived cross-reactive T help. *Eur. J. Immunol.* 1990. **20**: 2547–2554.

- 47 Altman, J. D., Moss, P. A., Goulder, P. J., Barouch, D. H., McHeyzer-Williams, M. G., Bell, J. I., McMichael, A. J. and Davis, M. M., Phenotypic analysis of antigen-specific T lymphocytes. *Science* 1996. **274**: 94–96.
- 48 Gallimore, A., Glithero, A., Godkin, A., Tissot, A. C., Pluckthun, A., Elliott, T., Hengartner, H. and Zinkernagel, R., Induction and exhaustion of lymphocytic choriomeningitis virus-specific cytotoxic T lymphocytes visualized using soluble tetrameric major histocompatibility complex class I-peptide complexes. *J. Exp. Med.* 1998. **187**: 1383–1393.
- 49 Prat, M., Gribaudo, G., Comoglio, P. M., Cavallo, G. and Landolfo, S., Monoclonal antibodies against murine gamma interferon. *Proc. Natl. Acad. Sci. USA* 1984. **81**: 4515–4519.
- 50 Oehen, S. and Brduscha-Riem, K., Differentiation of naive CTL to effector and memory CTL: correlation of effector function with phenotype and cell division. *J. Immunol.* 1998. **161**: 5338–5346.
- 51 Kraal, G. and Janse, M., Marginal metallophilic cells of the mouse spleen identified by a monoclonal antibody. *Immunology* 1986. **58**: 665–669.
- 52 Bachmann, M. F., Odermatt, B., Hengartner, H. and Zinkernagel, R. M., Induction of long-lived germinal centers associated with persisting antigen after viral infection. *J. Exp. Med.* 1996. **183**: 2259–2269.